

Structural interpretation of the deepwater Gunashli Field, facilitated by 4-C OBS seismic data

DOMINIC M. MANLEY, SEAN F. MOHAMMED, and NIGEL D. ROBINSON, BP, Sunbury on Thames, UK
ROWLAND W. THOMAS, Consultant, BP, Sunbury on Thames, UK

The ACG Field (Azeri, Chirag, Gunashli) was discovered by the State Oil Company of the Azerbaijan Republic (SOCAR). Since 1980 SOCAR has been producing oil from the northwest end of the structure, known as Shallow Water Gunashli (SWG). In 1994 the Azerbaijan International Oil Company (AIOC) signed a 30-year Production Sharing Agreement (PSA) with the state. AIOC began production from the central part of the field, Chirag, in late 1997. Chirag currently produces approximately 140 000 b/d. Azeri achieved first oil in early 2005. Development drilling will start at DWG in late 2005 with first oil due in 2008. BP now operates on behalf of the AIOC partners

The reservoir at ACG comprises a stack of Plio-Pleistocene lacustrine-deltaic sandstones, sourced from the north by the paleo-Volga River system. The main reservoirs are the Pereriv B and D sandstones. These are sheet sandstones with average thicknesses of 42 and 30 m, respectively. These lie between 2300 and 4700 m within the PSA, with oil-water contacts typically between 3000 and 3450 m. Overlying the Pereriv are the more channelized, secondary reservoirs of the Balakhany formation. The structure is a high-amplitude, thrust anticline, aligned northwest to southeast, approximately 50 km in length and up to 5 km in width. Structural dips on the flanks vary between 20 and 80°. The structure is penetrated from deeper levels by several mud volcanoes.

Seismic coverage and data quality. Since 1995, four 3D seismic surveys have been acquired over all or part of ACG. Figure 1 shows a September 2002 map of the full ACG field with the surveys outlined. In 1995, a 3D survey was acquired to meet the minimum work program of the PSA and to support first oil production at Chirag. In 2002, a repeat towed-streamer 3D survey was acquired to monitor fluid movement at Chirag. The 2002, 4-C OBS 3D surveys were designed to overcome specific imaging problems at Azeri and DWG to reduce uncertainty during the predrill programs in these two areas. Figure 2 shows the DWG structure with the key horizons.

The 4-C OBS PZ compressional-wave data have improved the image of the structure. However, processing the 4-C OBS converted-wave data has proved problematic. Interim results from the converted-wave data are encouraging in some parts of DWG, but it has not yet been possible to produce a consistently imaged data set which would support interpretation and supersede the compressional-wave image. Consequently, this paper concentrates upon the interpretation of the products of the PZ summation compressional-wave processing project and comparison of those products with the 2002 3D towed-streamer data.

Figure 3 compares towed-streamer and 4-C OBS PZ images of the DWG structure. Figure 4 shows the signal-to-noise calculated at the Pereriv reservoir level on both data sets. Figure 3 also demonstrates the superior image quality offered by the PZ data. Good reflector continuity is seen across the southern flank of the structure (between the two bounding faults), whereas the streamer data are difficult to interpret in this area. The south flank of the structure is now imaged as a laterally unbroken reflector. Previous interpre-

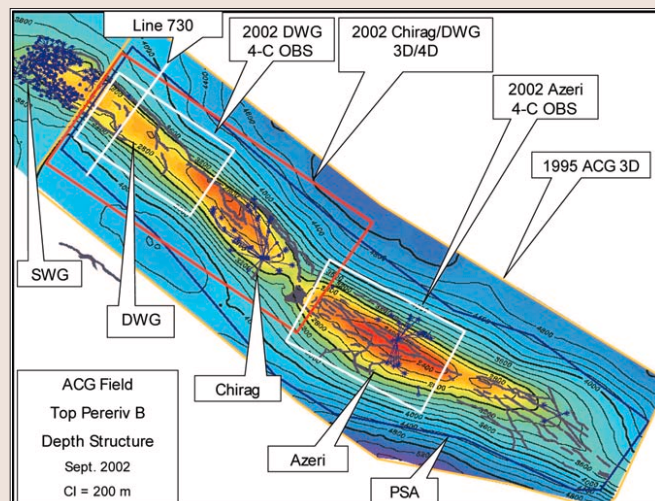


Figure 1. ACG seismic database. This shows the key surveys overlaid on a Top Pereriv B structure map from 2002. Other surveys such as older 2D data and high-resolution site survey data also exist.

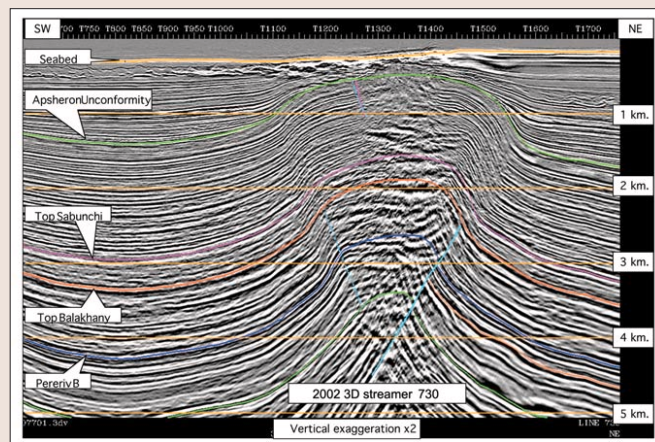


Figure 2. 2002 3D streamer line 730 showing the main features of the DWG structure. Note the noise contamination at the crest of the structure due to the gas cloud.

tations often showed strike parallel faults which coincided with changes in data quality in the overburden. These faults are not evident on the PZ image, and this reduces risk on crestal compartmentalization. In general, where the PZ data are well-imaged there appears little or no seismic scale faulting between the two main bounding faults. Figure 5 further reinforces this impression, demonstrating that lateral continuity along the strike through the core of the structure is superior on the PZ data.

The superior quality seen in the 4-C OBS PZ data is attributed to the following:

- sensor deployment in a quiet, ocean floor environment, allowing good coupling with the seabed
- wide-azimuth acquisition, enabling discrimination against overburden features that can potentially scatter energy
- high fold—the fold of the PZ data is up to 10 times that

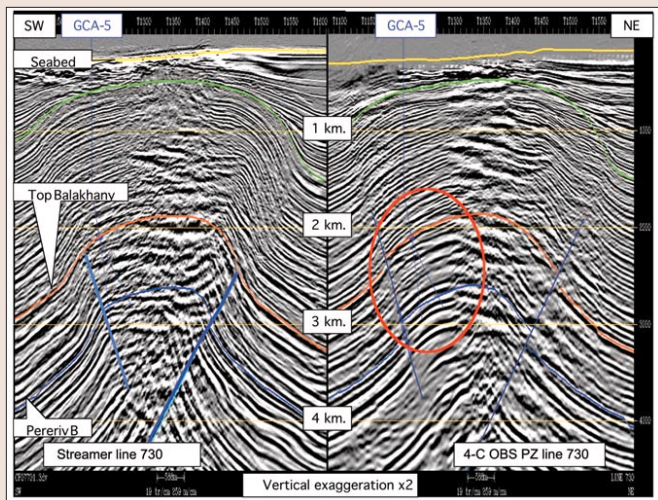


Figure 3. Comparison between streamer (left) and OBS PZ data (right). The south flank of the structure shows clear image improvement on the PZ data (circled in red).

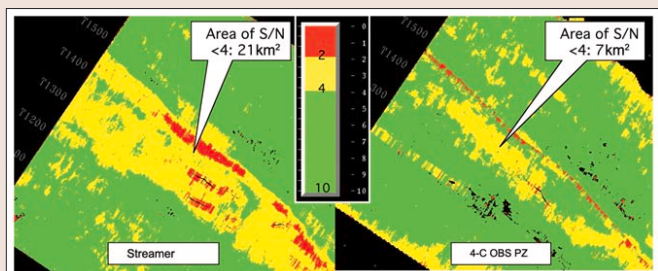


Figure 4. Comparison of signal-to-noise ratio on streamer and 4-C OBS PZ data. The area of S/N lower than four has been significantly reduced. Green signifies areas of moderate or good data. Yellow indicates where amplitudes are attenuated and frequently uninterpretable. Red usually shows areas of very poor data or highlights faults.

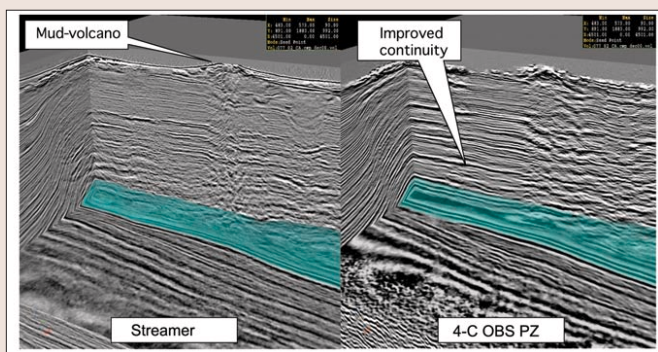


Figure 5. Chair display comparing strike continuity of reflectors on streamer and 4-C OBS PZ data. The Top Pereriv B surface is in pale blue.

- of the streamer data, enabling a boost in signal-to-noise
- PZ summation, enabling receiver-side water-bottom multiple attenuation

The same causes and effects were observed in the Azeri 4-C OBS survey PZ data. The processing of the DWG PZ data is described by Bouska et al. in this issue.

Interpretation. The depth-migrated data were delivered in the uncalibrated depth domain. Reflectors do not respect well-depths in this data set. The following steps were taken to tie the seismic horizons to the well control:

- The processing velocity model was used to stretch the

uncalibrated depth seismic data to time.

- Synthetic seismograms and VSP data were used to ensure the correct picking position for the key horizons.
- The time ties were stretched back to uncalibrated depth.
- The key horizons were picked on the uncalibrated depth data. Picking was performed in depth in order to maintain the correct dip and thickness relationships.

The uncalibrated depth data were calibrated to the wells using a residual-scaling method, explained later.

Six horizons were interpreted on the uncalibrated depth data (Figure 6). The crestal area of the DWG structure is still poorly imaged on the PZ data due to the gas cloud. Consequently, the elevation of the reservoir was estimated where it is not imaged. To achieve this, geometric reconstruction principles were used to build the interpretation downward from the shallowest horizons. This approach was guided by the depositional model for the preunconformity section, prior to folding. The model assumes a very low angle slope with widespread isopachous sedimentation. This model, derived from core data sedimentological studies, infers that the prefolded structure should maintain reflector relationships which are subparallel and one where the tops and bases of units do not converge or diverge rapidly. Indeed much of the overburden, with the exception of the uppermost kilometer or so, does not show evidence of major or local unconformities.

The PZ data do demonstrate a section of approximately uniform thickness, in agreement with the depositional model. The towed-streamer data sets, by contrast, often show thickening into the synclines to the south and north. This did not agree with the depositional model as described above. The thickening seen in the streamer data was ambiguous. Either the data were correct and the depositional model wrong or the data were incorrect (possibly due to uncalibrated velocities off structure) and the depositional model was correct. This inconsistency has now been resolved with the delivery of the PZ data and the geologic and geophysical data are in better agreement. However, it must be recognized that the more uniform thickness seen in the PZ data is due to the velocity model that imaged them optimally and not due to the bottom-cable data acquisition technique.

Below the main unconformity (Figure 6), the horizons are interpreted as being subparallel where they are not well imaged. The key reflectors are seen to be discontinuous where they go into or below the gas cloud. Their dips and subparallel interrelationship were maintained as far as possible until they emerged from the gas cloud on the north flank of the structure. Even before the well-imaged reflectors disappear, they are often seen to be affected by push-down below discreet, bright gas-charged zones above and outside of the main gas cloud (Figure 7). This is compensated for by forcing the structural surfaces to depart from the correct pick position on the event at the point of where the push-down begins. A second set of interpreted horizons was also created which follows the reflectors directly. These horizons were used for attribute extraction.

It was initially thought that the data at the crest were degraded and affected by delay of primary energy. However, during processing of the PZ data, this view was changed to one where the crest is believed to be dominated by short-period multiple energy, evident in the prestack gathers, probably generated by a succession of gas-charged units. Thus, what was once picked as a delayed primary reflector, awaiting correction during depth calibration/conversion, is now corrected by the geometric reconstruction methodology described above. Despite the fact that some areas

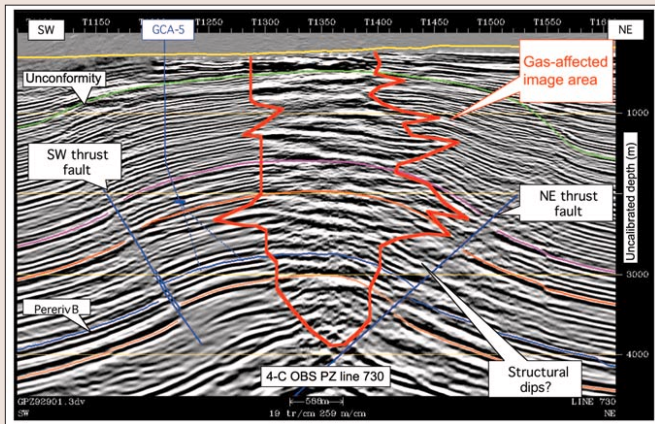


Figure 6. 4-C OBS PZ line 730, showing the key structural and interpretational features.

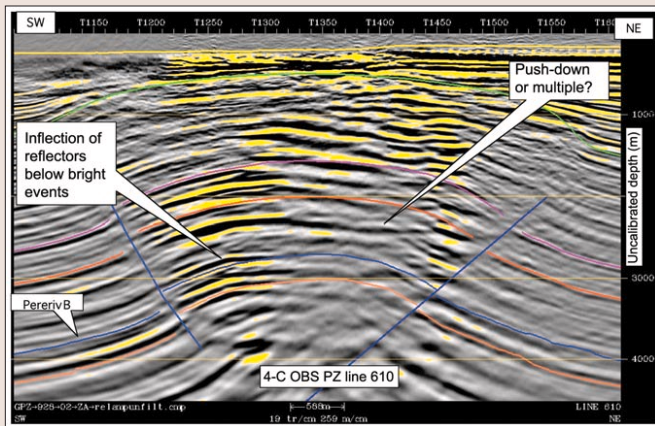


Figure 7. 4-C OBS PZ line 610, displayed with true relative amplitude, showing the brightest events highlighted in yellow.

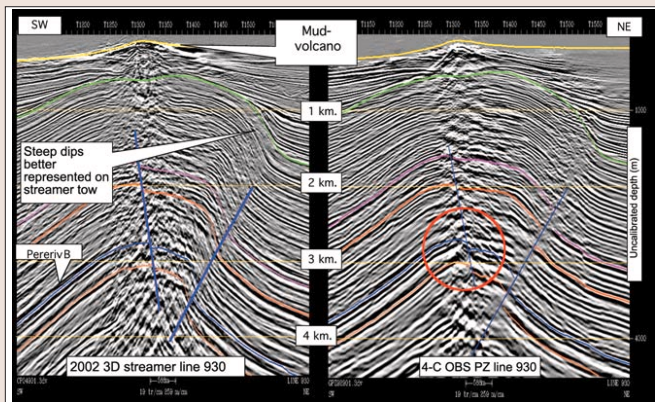


Figure 8. Comparison between streamer and 4-C OBS data at the location of the mud volcano between DWG and Chirag. The main area of improvement seen on the PZ data is circled in red.

remain unimaged, these are now much smaller than they were in the streamer area. The improvement in image is demonstrated in Figure 8, which shows a line through the mud volcano which is situated in the area between DWG and Chirag.

Aside from the configuration of the crest, the other key uncertainty is the location and throw of the bounding thrust faults. Figure 6 (line 730) shows the northeast and southwest verging thrust faults. These are believed likely to be fold accommodation faults resulting from tightening of the fold later in the structural history of DWG. The field will be developed by water flood from a number of down-flank

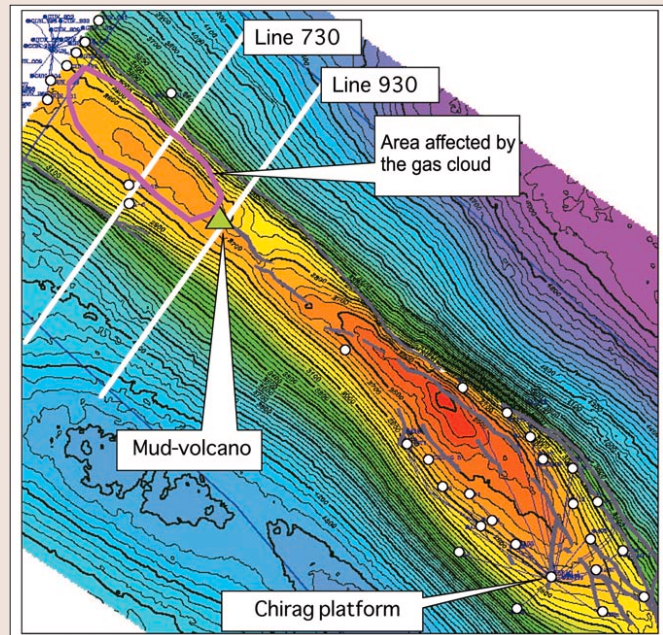


Figure 9. Top Pereriv B depth structure from 4-C OBS PZ data before calibration to wells. Well control points are highlighted by white circles.

injection wells. Thus it is vital to know where these main faults are located to optimize injector locations. The PZ data revealed the southwest verging fault to be some 300 m further southwest than it was imaged on the streamer data. This is believed to be a velocity/migration affect. The velocity field which best images the PZ data appears to be slower than that which best images the streamer data. The acquisition and processing of the PZ data have changed the view of uncertainty prior to the execution of the predrill development program. In some areas uncertainty has been reduced. In other areas uncertainty has remained unchanged. Recently, however, newly accessed SWG well data, offset from the northwestern PSA boundary, appear to confirm the fault locations as imaged by 4-C OBS PZ data to be more likely than those imaged by streamer data.

Having applied the geometric reconstruction style interpretational technique and located the top reservoir either at its correct picking position in well-imaged areas, or by prediction in poorly imaged areas, the Pereriv B can be mapped in the uncalibrated time domain. Figure 9 shows the map at the top of the Pereriv B.

Depth calibration. Six structural surfaces were available in the uncalibrated depth domain. The following steps were taken to calibrate the data-to-well control points:

- calculation and mapping of residuals between raw depth and wells at six horizons
- calculation of scalar grids relating calibrated to uncalibrated depth
- use of the scalar grids to create a scalar seismic trace volume
- generation of an average velocity seismic trace volume from the processing velocities
- multiplication of the average velocity trace volume by the scalar trace volume
- generation of a well-calibrated time-to-depth model from scaled velocity trace volume
- conversion of the uncalibrated horizons, faults and seismic to well-calibrated depth through the new, scaled time/depth model

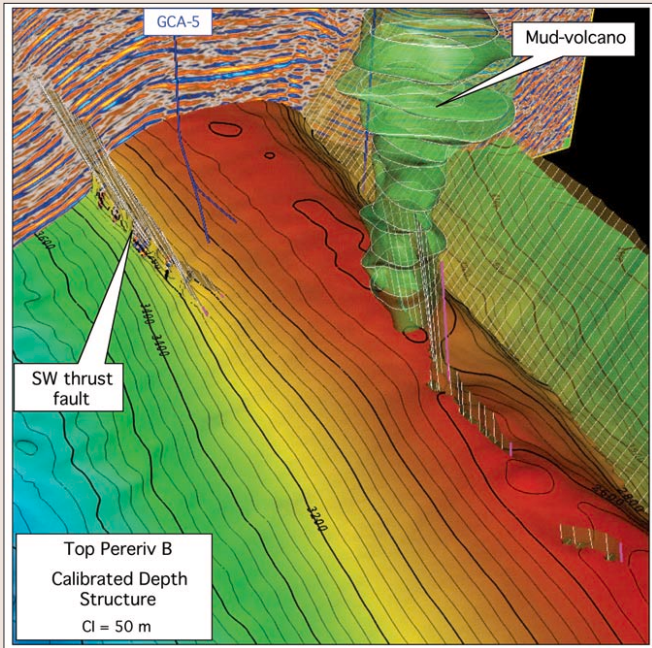


Figure 10. 3D view of the Pereriv B from the southeast.

The surfaces were then available in the calibrated depth domain for geologic model building. Figure 10 shows the DWG structure viewed in 3D from the southeast.

Application of technology. A range of modern geophysical technologies have been applied at DWG to reduce uncertainty. These include:

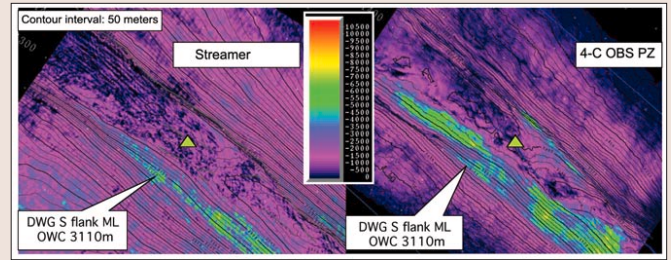


Figure 11. Pereriv B maximum trough amplitude calculated from inverted volumes from streamer (left) and 4-C OBS PZ (right).

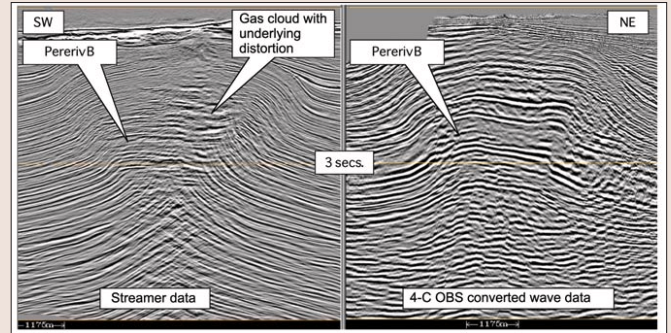


Figure 12. Comparison between streamer PreSDM data and 4-C OBS converted-wave PreSTM data at the northwest end of the ACG structure. Both data sets have been stretched to P-wave time.

- Kirchhoff prestack depth migration (PreSDM)
- colored inversion—i.e., BP's in-house best practice technique for AI inversion (Lancaster and Whitcombe, 2000)
- spectral decomposition (Partyka et al., 1999)
- coherency

Of these, the two that have added value are PreSDM and colored inversion. PreSDM re-imaged the north flank of Chirag and identified several new drilling targets. It is expected that it will deliver similar value at DWG. Colored inversion has improved attribute analysis of the oil-water contact (OWC) on the south flank of DWG. Figure 11 shows the OWC highlighted by attribute extraction from inverted PZ data and compared with the equivalent response from the streamer data.

Imaging the oil-water contact.

The OWC has not been penetrated on the south flank of DWG. The most likely OWC is currently estimated from actual contacts at Chirag and SWG. The OWC imaged by PZ attributes is consistent with the interpreted "most likely" OWC.

Amplitudes derived from PZ data are stronger in the oil-leg than on streamer data and show greater contrast between water and oil amplitudes.

These results have led to a better definition of the OWC. However, in the crest of the structure the seismic amplitudes are attenuated below the gas cloud. The amplitude maps (Figure 11) show dim areas in the crest although they are expected to be hydrocarbon-bearing.

Converted-wave results. Processing the converted-wave (PS) component of the 4-C OBS data set has proved challenging. At this time these data have not yielded a final result which can be used as a standalone product to support interpretation. Nevertheless there has been considerable encouragement from intermediate products which suggest that further processing work will eventually deliver PS volumes which could supersede compressional seismic images. In localized areas the PS imaging is revealing the true structural shape of DWG (Figures 12 and 13).

Good-quality PreSTM PS imaging is confined to the extreme northwest of the survey area. It was expected that depth processing would further improve the image and extend the area of interpretable PS imaging further south. This expectation has not so far been borne out. However, the PS depth image has proved useful in the northern part of the survey. Figure 13 shows the PS depth data overlain by the horizons as interpreted on the PZ data set.

Figure 13 demonstrates that there is a good correlation between the structure as imaged by PZ and converted-waves, using independently derived velocity models. This increases the confidence in the PZ data and the interpretation which is being used to support the field development.

Conclusions. Interpretation of the 4-C OBS PZ data at DWG has significantly improved confidence in the understanding of the structure and fluid contacts. The key results are:

- The size of the poorly imaged area has been reduced, and the confidence in the mapping is over a much larger area.

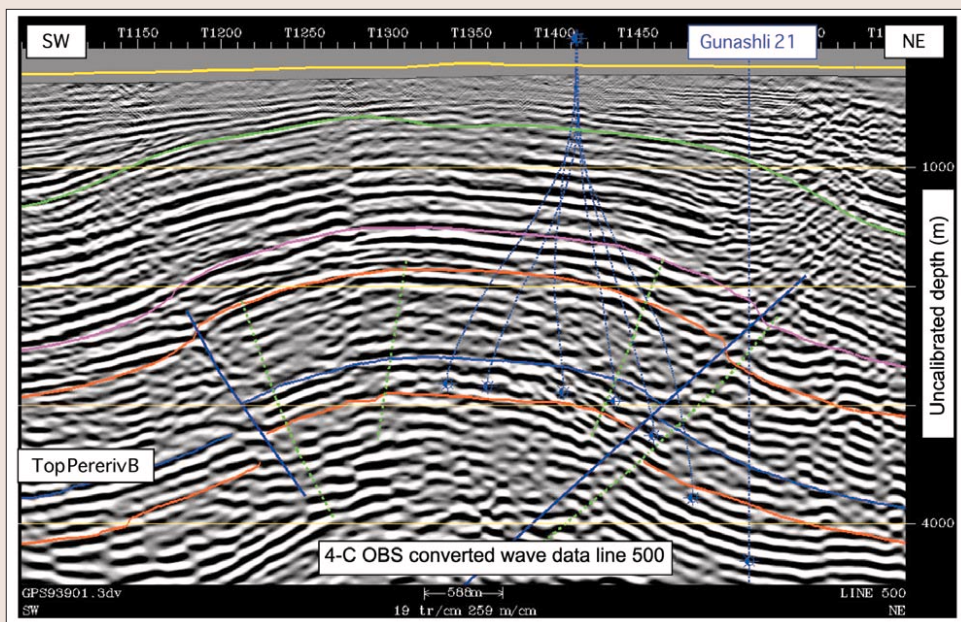


Figure 13. 4-C OBS converted-wave PSDM line 500. PZ interpreted horizons are overlaid on the PS data. Good correspondence of structural form is seen between the PZ horizons interpreted by the geometrical reconstruction method and PS data.

- The isopach maps are more consistent with the depositional model than previous seismic data sets.
- Positioning of the southwest verging thrust fault now agrees with that confirmed by dense well-control outside the PSA to the northwest.
- The image contributes to the understanding of a structure with relatively simple internal geometry and a likely lower risk of internal compartmentalization.
- Better signal-to-noise enables a cleaner image of the OWC on the south flank of the structure.
- The converted-wave image, where high-quality imaging exists, does not contradict the PZ interpretation and adds confidence in the true structural shape free of potential gas push-down effects.

Suggested reading. "Reducing structural uncertainty on the Azeri field using ocean bottom seismic: offshore Azerbaijan" by Lyon et al. (SEG 2004 *Expanded Abstracts*). "Fast-track 'colored' inversion" by Lancaster and Whitcombe (SEG 2000 *Expanded Abstracts*). "Interpretational applications of spectral decomposition in reservoir characterization" by Partyka et al. (TLE, 1999). TJE

Acknowledgments: The authors thank BP management and the AIOC partners for permission to publish this case study. We also acknowledge the skill and dedication of Caspian Geophysical and WesternGeco who acquired and processed the DWG 4-C OBS survey respectively. Within BP many colleagues contributed to the successful outcome of this project. They included Jack Bouska, Dave Buddery, Alan Ford, Dave Howe, John Howie, Rodney Johnston, Thomas Lyon, Mike Mueller, Martin Riviere and Richard Seabourne. Furthermore we thank Phil Hicken and Geoff Troop of Landmark Graphics Corporation for their support of the interpretation.

Corresponding author: dominic.manley@uk.bp.com